茨城県立医療大学紀要　第24巻
A S V P I Volume 24

Original Article

Radioiodinated 6-iodo-D-*meta*-tyrosine: Characterization of Uptake in DLD-1 Colon Cancer Cells and Biodistribution in Mice

Naoto Shikano[1)], Nobuyuki Yagi[1)], Ryuichi Nishii[2)], Kazuyo Ohe[3)], Syuichi Nakajima[1)], Masato Ogura[1)], Ayako Ikeda[1)], Masato Kobayashi[3)], Naoto Yamaguchi[4)], Keiichi Kawai[3)]

[1)]Department of Radiological Sciences, Ibaraki Prefectural University of Health Sciences
[2)]Diagnostic and Therapeutic Nuclear Medicine Team Department of Molecular Imaging and Theranostics, National Institute of Radiological Science
[3)]Division of Health Science, Graduate School of Health Sciences, Kanazawa University
[4)]Center for Medical Science, Ibaraki Prefectural University of Health Sciences

Abstract

Introduction: ^{123}I-6-iodo-D-*meta*-tyrosine (^{123}I-6-D-*m*Tyr) is an iodine-labeled D-amino acid employed potentially in molecular imaging of tumors. We used its ^{125}I-labeled analogue (6-I-D-*m*Tyr), which has a long half-life and is suitable for basic studies, to examine the mechanism of ^{123}I-6-D-*m*Tyr accumulation in DLD-1 human colon cancer cells and its biodistribution in normal mice.

Methods: DLD-1 cells (5.0×10^5) suspended in 5 ml of culture medium (Dulbecco`s Modified Eagles Medium) containing fetal bovine serum and L-glutamine were seeded into 6-cmφ culture dishes and cultured at 37°C, CO_2 5%, and pH 7.4. Time curves for the uptake of 6-I-D-*m*Tyr (18.5 kBq) into DLD-1 cells were constructed, and the transport systems were analyzed by uptake-inhibition experiments using 2-amino-bicyclo[2,2,1]heptane-2-carboxylic acid (a system L–specific inhibitor) and 2-(methylamino)isobutyric acid (a system A–specific inhibitor) at an uptake temperature of 4°C. Also, 6-I-D-*m*Tyr (11.1 kBq) was administered to male ddY mice (6 weeks old) by injection into the tail vein, and the time-course of its biodistribution was determined.

Results*:* The uptake of 6-I-D-*m*Tyr into DLD-1 cells peaked at 10 min. Membrane transport inhibition studies indicated that ca. 70% of the incorporated amount was due to membrane transport (ca. 50% was due to transport system L, and the other ca. 20% was due to membrane transport via an unknown mechanism), whereas inhibition unsaturated uptake was estimated to be ca. 30% (4°C). Physiologic accumulation of 6-I-D-*m*Tyr in normal mouse tissues was low overall, and clearance from the blood was observed to be rapid. Accumulation in the stomach was also low, indicating excellent metabolic resistance to de-iodination enzymes.

Conclusions*:* In normal mice, the concentration of 6-I-D-*m*Tyr in organs and tissues decreased rapidly following administration, whereas in DLD-1 mice, both the uptake and retention of 6-I-D-*m*Tyr were excellent. These results highlight the potential of 6-I-D-*m*Tyr as a new labeling agent for use in molecular imaging of tumors.

Key words: 6-iodo-D-*meta*-tyrosine, system L, neutral amino acid, DLD-1 cells

Address: Naoto Shikano. Department of Radiological Sciences, Ibaraki Prefectural University of Health Sciences, 4669-2 Ami, Ami-machi, Inashiki-gun, Ibaraki 300-0394, Japan
Phone: +81-29-840-2217, Fax: +81-29-840-2317, E-mail address: sikano@ipu.ac.jp

1. Introduction

It is well known that, depending on the optical isomer, the biological affinity of drugs often differs significantly. The same can be said in regard to the optical isomers of natural and non-natural amino acids (AAs). D-AAs are not common compared with L-AAs. For that reason, much remains unclear regarding the affinity of D-AAs and their analogues for intermediates of biological pathways, and recent years have seen an upsurge in research on D-AAs in the field of radiopharmaceuticals.

Our first attempt to use a D-AA as a diagnostic radiopharmaceutical was reported by our co-authors, Kawai et al., who developed ^{125}I-3-iodo-D-tyrosine (3-^{125}I-Tyr) as a diagnostic agent for amino acid membrane transport in the pancreas.[1] Langen et al. reported that accumulation of the D-isomer of cis-4-[^{18}F]fluoro-proline in the human brain parenchyma was 5 times greater than that of the L-isomer, an interesting finding that at first glance would seem to go against expectation.[2]

From the standpoint of using the D-isomers of natural AAs, it was reported that with ^{14}C-methionine[3] and ^{14}C-leucine[4], the D-isomers are more highly accumulated than L-isomers in the pancreas and transplanted tumor cells. Also, we investigated the uptake of a number of natural AAs and their respective optical isomers in Chinese hamster ovary-K1 (CHO-K1) cells.[5] We found that ^{14}C-D-phenylalanine, ^{14}C-D-alanine, ^{14}C-D-methionine, and ^{14}C-D-leucine and their L-isomers accumulated at comparably high levels in cells, and the L-isomers of ^{14}C-serine, ^{14}C-valine, ^{14}C-tyrosine, ^{14}C-glutamine, and ^{14}C-arginine showed high stereo-selectivity in regard to accumulation in CHO-K1 cells.[5]

There have also been a number of reports regarding the uptake of non-natural D-AAs in tumors. In tumor-bearing animals, minimal difference was observed with respect to the accumulation of 2-iodo-D-phenylalanine and its L-isomer according to the optical isomer in normal tissues, but 2-iodo-D-phenylalanine's accumulation in tumors was lower than that of the L-isomer.[6] However, a study in normal humans found that, compared with the L-isomer, the D-isomer was rapidly cleared from the blood and excreted in the urine, indicating greater suitability for tumor imaging.[7] Also, it was reported that the D-isomers for a number of AAs, including *O*-^{11}C-methyl tyrosine, *O*-^{18}F-fluoromethyl tyrosine, *O*-^{18}F-fluoroethyl tyrosine, *O*-^{18}F-fluoropropyl tyrosine, and ^{11}C-methionine, showed lower uptake by tumors than the L-isomers, but their tumor/blood and tumor/normal tissue ratios (that is, the contrast between the tumors and the background) were superior.[8,9] An *in vitro* study found that, compared with *O*-^{18}F-L-fluoroethyl tyrosine, the D-isomer accumulated only minimally in human colon cancer cells,[10] and the D-isomer also showed almost no accumulation in mouse brain.[11] Schober et al.[12] reported similar accumulation of L- and D-^{11}C-methionine in a malignant glioma, whereas Bergström et al.[13] found that accumulation of D-^{11}C-methionine into brain tumor was lower than that of L-^{11}C-methionine. More recently, our basic study found that D-^{3}H-methionine accumulated in human-derived cultured tumor cells as result of transport by systems L and ASC, whereas L-^{3}H-methionine was transported by system L; in mice bearing transplanted tumors, D-^{3}H-methionine accumulation was significantly higher than that of L-^{14}C-methionine.[14]

We carried out a series of studies using radioactive iodine–labeled compounds, including *meta*-tyrosine, with the ultimate objective of developing a diagnostic imaging agent for use in positron emission tomography (PET) and single-photon emission computed tomography (SPECT).[5,14–18] In the present study, we focused on ^{125}I-6-iodo-D-*meta*-tyrosine (6-I-D-*m*Tyr) (Fig. 1), the D-isomer of iodine-labeled *meta*-tyrosine. We investigated the accumulation of 6-I-D-*m*Tyr in DLD-1 colon cancer cells[19] and the expression of AA transporters and determined the biodistribution in mice.

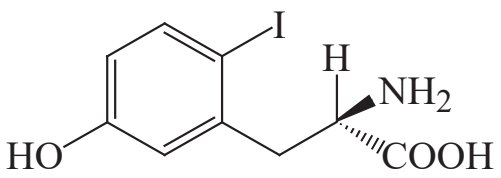

Fig. 1. Structure of 6-iodo-D-*meta*-tyrosine (6-I-D-*m*Tyr).

2. Materials and Methods

2.1. Materials

The radiolabel precursor (D,L-*m*Tyr) was purchased from Sigma-Aldrich Japan Co. ^{125}I-NaI was purchased from Amersham Pharmacia Biotech. D-[^{14}C(U)] tyrosine was purchased from American Radiolabeled Chemicals Inc. DLD-1 (human colon adenocarcinoma, JCRB9094) cells were purchased from JCRB. Plastic tissue culture dishes (diameter 6 cmφ, Cat. no. 150288) and plastic culture flasks (surface area 25 cm^2, Cat. no. 163371) were purchased from Nalge Nunc International. 2-Amino-bicyclo[2,2,1]heptane-2-carboxylic acid (BCH, a system L–specific inhibitor), 2-(methylamino)isobutyric acid (MeAIB, a system A–specific inhibitor), natural L/D-amino acids, and other chemicals of reagent grade were purchased from Kanto Chemical Co., Inc.

2.2. Labeled Amino acids

We separated L-*m*Tyr from D,L-*m*Tyr using high-performance liquid chromatography (HPLC) with a Crownpak CR(+) chiral column (Daicel Chemical Industries, Ltd.). Separated L-*m*Tyr was labeled with ^{125}I-NaI (8.1×10^{19} [Bq/mol]) and Chloramine-T (Kanto Chemical Co., Inc.). Radioiodination of D-*m*Tyr produces 2 major geometric isomers: 6-iodo- and 4-iodo-D-*m*Tyr.[16] To separate and purify these 2 isomers, we performed HPLC with a Nova-Pak C18 column (Waters Co.). Radiochemical yield was checked using a silica gel thin-layer chromatography kit (Merck). The labeled compounds were used in their noncarrier-added condition.

2.3. Cell Culture and Proliferation Curves

DLD-1 cells (10^5 cells/ml) were incubated in 6-cm dishes with 5 ml of Dulbecco's modified Eagle's medium (Cat. no. D5796, Sigma Chemical Co., St. Louis, MO, USA) containing 10% fetal calf serum at 37°C in a 5% CO_2 atmosphere (pH 7.4). Sub-culturing was performed every 5 days using 0.02% ethylenediamine tetraacetic acid and 0.05% trypsin.[5] DLD-1 cells were seeded on 60-mm dishes at a density of 5×10^5 cells in 5.0 ml of the complete culture medium. The growth curve was plotted based on growth up to 6 days after inoculation. Cells were used for experiments on the 3rd or 4th day after inoculation.[5] Cell proliferation curves were prepared to determine the duration of the logarithmic growth phase.

2.4. Time Course of 6-^{125}I-D-mTyr Uptake

When DLD-1 cells had been cultured to a density of about 80% confluence (3-4 days after inoculation), the medium was replaced with 5 ml of phosphate-buffered saline (PBS) containing Na^+ (37°C, pH 7.4). The cells were then incubated at 37°C for 10 min. Next, the PBS was replaced with 2.0 ml of uptake solution containing 18.5 kBq of 6-I-D-mTyr. The incubation was conducted using PBS with Na^+ uptake solution (NaCl, 137 mM; KCl, 3.7 mM; Na_2HPO_4, 8.0 mM; KH_2PO_4, 1.5 mM; $CaCl_2\cdot2H_2O$, 1.8 mM; $MgCl\cdot6H_2O$, 1 mM). The cells were then incubated for 5, 10, 15, 30, and 60 min. Next, the medium was removed, and the cells were then washed twice using 5.0 ml of cold PBS and solubilized using 2.0 ml of NaOH (2 N). The radioactivity of each aliquot (500 ml) was counted using an auto-well counter (Aloka, Japan; ARC-380). The result for each set of experimental conditions was the mean of 4 dishes.

2.5. Labeled Amino Acid Uptake Inhibition Study

In the analysis of transport system L, we removed the culture fluid from the culture dishes, added 5 ml of 37°C PBS, and incubated the dishes for 10 min at 37°C, 5% CO_2, and pH 7.4. The PBS was then removed. To investigate the concentration dependence of uptake, we added 0.1, 0.5, 1.0, 5.0, and 10.0 mM BCH as a specific transport system inhibitor to 5 ml of 37°C Na^+-free PBS containing 18.5 kBq of carrier-free 6-I-D-*m*Tyr (137 mM choline-Cl, 3.7 mM KCl, 8.0 mM K_2HPO_4, 1.5 mM KH_2PO_4, 1.8 mM $CaCl_2\cdot2H_2O$, 1 mM $MgCl\cdot6H_2O$) as an uptake solution. The dishes were again incubated for 10 min under the conditions described above. The uptake solution was removed, and the cell surface was rinsed two times with 5 ml of ice-cold PBS. In addition, 2 ml of NaOH (2 N) was added, and the dishes were left standing at room temperature for 24 h to solubilize the cells. The radioactivity in an aliquot (500 µl) of each sample was measured.

In the analysis of transport system A, PBS with Na^+ was

used as the uptake solution, with the specific transport system inhibitor MeAIB at 0.1, 0.5, 1.0, 5.0, and 10.0 mM to examine the concentration dependence of uptake. The specific transport system inhibitor concentration dependence was determined based on the radioactivity levels recorded in the above experiments, and analysis of the transport system was carried out at the concentration showing the greatest inhibitory effect.

We examined the system L specificity of transport of the labeled amino acids in DLD-1 cells. One of the following compounds was added to cell cultures at a final concentration of 10 mM or 1 mM: BCH in incubation medium without Na^+; or 1 mM MeAIB in incubation medium with Na^+. The cells were then incubated in 2 ml of incubation medium with/without Na^+ containing 18.5 kBq of 6-I-D-*m*Tyr or D-[^{14}C(U)] tyrosine for 10 min at 37°C. In the medium without Na^+, NaCl was replaced with the same concentration of choline-Cl. To examine effects of low temperature, we incubated cells for 10 min at 4°C. We measured the radioactivity associated with solubilized cells using an ARC-380 well-type scintillation counter (Aloka) for ^{125}I-labeled compounds and an LS6500 liquid scintillation counter (Beckman Instruments, Fullerton, CA, USA) for ^{14}C-labeled compounds.

2.6. qRT-PCR Analysis of DLD-1 Cells

Total RNA was harvested from each tumor cell using an RNeasyb Mini kit (Qiagen K. K, Tokyo, Japan). The quality of the total RNA was evaluated using a bioanalyzer (Agilent Technologies, Santa Clara, CA, USA). Complementary DNA (cDNA) was amplified only from high-quality total RNA using an AffinityScript qRT-PCR cDNA Synthesis kit (Agilent Technologies). The thermal profile of the reaction was as follows: 5 min at 25°C for 1 cycle, 15 min at 42°C for 1 cycle, and 55 min at 95°C for 1 cycle. The genes analyzed by qRT-PCR were Na^+-independent transport L systems (*LAT1*, *LAT2*, *LAT3*, *LAT4*) and *4F2hc*. Two different housekeeping genes, glyceraldehyde-3-phosphate dehydrogenase (*GAPDH*) and beta actin (*ACTB*) were used as internal controls to compensate for the differences between the initial RNA and cDNA amounts. An Mx3005P thermocycler (Agilent Technologies) was used for the qRT-PCR reactions. Primers (Table 1) were synthesized by Nihon Gene Research Laboratories, Inc. (Miyagi, Japan). The artificial plasmid used for the calibration curve was synthesized by GenScript (Piscataway, NJ, USA). The qRT-PCR reagent used in this study was Brilliant II Fast SYBR Green qRT-PCR Master Mix (Stratagene Products Division, Agilent Technologies). The thermal profile of the reaction was as follows: 2 min at 95°C for 1 cycle, 5 s at 95°C followed by 20 s at 60°C for 40 cycles, 1 min at 95°C followed by 30 s at 55°C and 30 s at 95°C for 1 cycle. In addition, serial dilutions of artificial plasmids were performed. The samples used were created using a dilution series ranging from 1×10^2 to 1×10^8 copies per tube for the calibration curve. All reactions were performed in triplicate.

Table 1. Primers for real-time PCR.

	Primer	*Sequence* (5'-3')
4F2hc	Forward	taccggggtgagaactcgt
	Reverse	cagccaaaactccagagcat
LAT1	Forward	gtggaaaaacaagcccaagt
	Reverse	gcatgagcttctgacacagg
LAT2	Forward	ttgccaatgtcgcttatgtc
	Reverse	ggagcttctctccaaaagtcac
LAT3	Forward	tttggtggcatctgcctaa
	Reverse	attaacgtggagcgcaggt
LAT4	Forward	cagggagaccctctgtgg
	Reverse	cggtagcagatcaggtagagc
ACTB	Forward	ccaaccgcgagaagatga
	Reverse	ccagaggcgtacagggatag
GAPDH	Forward	agccacatcgctcagacac
	Reverse	gcccaatacgaccaaatcc

2.7. Biodistribution Study in Mice

In vivo experiments were performed to investigate the biodistribution of 6-I-D-*m*Tyr administered to mice. For 3-5 male ddY mice (6 weeks old) in each group, 0.1 ml of saline containing 11.1 kBq of 6-I-D-*m*Tyr was injected

into the tail vein. Animals were anesthetized with ether and sacrificed by heart puncture at 2, 5, 10, 15, and 30 min after the injection. They were dissected and the brain, heart, lung, liver, pancreas, spleen, kidney, stomach, and intestines were removed and weighed. Blood was also sampled. The radioactivity in each organ was determined using a well-type scintillation counter (ARC-300; Aloka). The biodistribution of the radioactivity was determined for each organ as percent dose/organ and on a per-organ-weight basis as percent dose/g.

2.8. Statistical Analysis

Data were collated as mean ± standard deviation of 3-5 measurements, and each experiment was performed in duplicate. Results were analyzed using the Student's *t* test. Probability levels of $P<0.0001$ were considered to indicate statistical significance.

3. Results

3.1. Cell Culture and Proliferation Curves

The cells showed continuous logarithmic growth beginning on Day 1 after seeding into the culture dishes (Fig. 2), and confluent growth was seen on Day 4. The number of cells decreased thereafter. Therefore, the cells were used in experiments on Day 3 after seeding.

3.2. Time Course of 6-^{125}I-D-mTyr Uptake

When the dishes were incubated for 10 min, 6-I-D-*m*Tyr uptake was 5.58±0.35%, and thereafter, 6-I-D-*m*Tyr was gradually washed out of the cells (Fig. 3). As a result, it was decided that the transport system analyses using a specific transport system inhibitor would be conducted at 10 min after administration of the labeled compound.

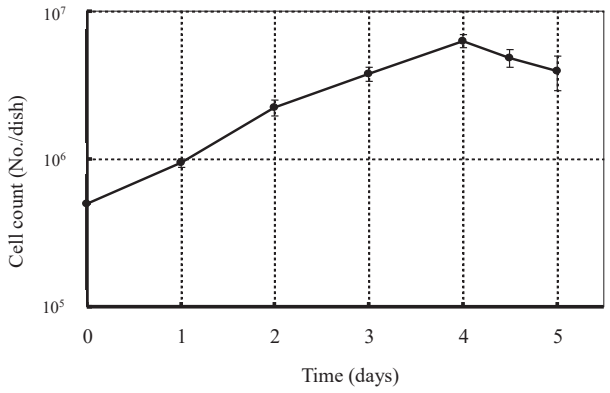

Fig. 2. Growth curve of DLD-1 cells.

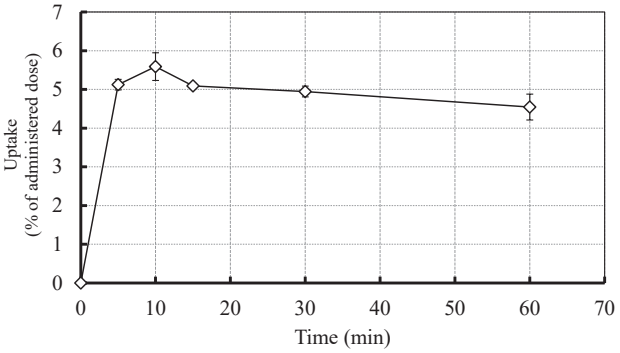

Fig. 3. Time course of 6-I-D-*m*Tyr uptake.

3.3. Labeled Amino Acid Uptake Inhibition Study

Inhibition of transport system L was dependent on the concentration of the inhibitor, and maximum inhibition was seen at 10 mM (Fig. 4-A). Based on that result, we analyzed transport system L using a BCH concentration of 10 mM.

Inhibition of transport system A was not dependent on the concentration of the inhibitor. There were some concentrations at which increased uptake was observed, but there were no statistically significant differences (Fig. 4-B). We analyzed transport system A at the MeAIB concentration that showed the greatest inhibitory effect, 1 mM.

The contribution of transport system L to the uptake of 6-I-D-*m*Tyr was 54.0±1.0%, which was statistically significant ($P<0.001$). The contribution of transport system A to 6-I-D-*m*Tyr uptake was 6.0±6.0%, which was not statistically significant ($P=0.561$) (Fig. 4-C). The contribution of transport system L to the uptake of [^{14}C(U)] D-tyrosine was 70.0±6.0%, which was statistically significant ($P<0.001$). The contribution of transport system A to [^{14}C(U)]D-tyrosine uptake was 3.0±3.1%, which was not statistically significant (Fig. 5). The uptake of both [^{14}C(U)]D-tyrosine and 6-I-D-*m*Tyr occurred via similar transport systems.

3.4. qRT-PCR Analysis of DLD-1 Cells

The expression of amino acid transport system genes in

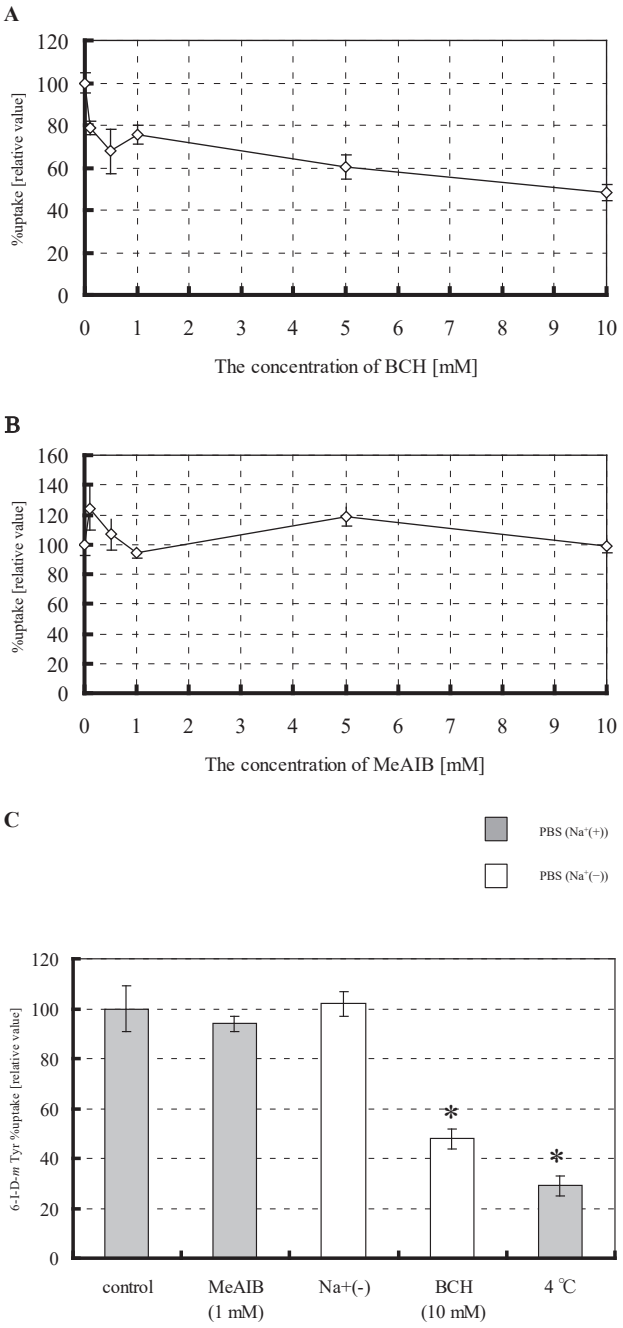

Fig. 4 (A) Curve demonstrating concentration-dependent inhibition of 6-I-D-*m*Tyr uptake by BCH.
(B) Curve demonstrating concentration-dependent inhibition of 6-I-D-*m*Tyr uptake by MeAIB.
(C) The effect of inhibitors (MeAIB, BCH) on 6-I-D-*m*Tyr uptake into DLD-1 cells incubated at 4°C in Na^+-free medium. Values represent mean ± SD as percent of administered dose (n = 4). *; $P<0.0001$ (statistical significant).

DLD-1 cells was analyzed using qRT-PCR. The high quality of the total RNA harvested from each tumor cell was confirmed using a bioanalyzer (data not shown). The expression levels of neutral amino acid transport system genes were calculated using a calibration curve for each

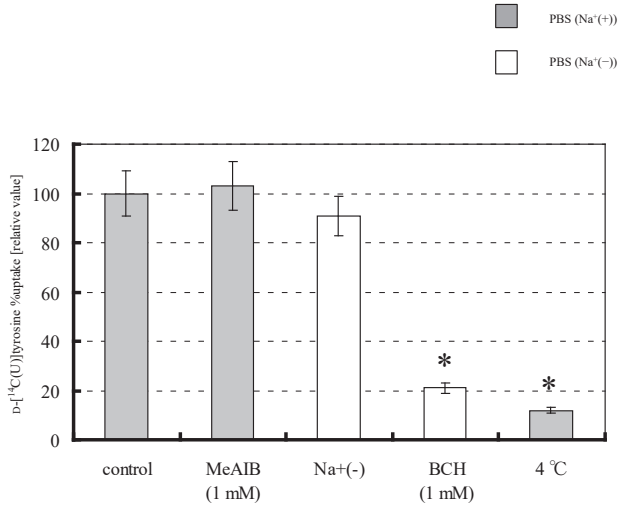

Fig. 5. The effect of inhibitors (MeAIB, BCH) on D-[^{14}C(U)] tyrosine uptake into DLD-1 cells incubated at 4°C in Na^+-free medium. Values represent mean ± SD as percent of administered dose (n = 4). *; $P<0.0001$ (statistical significant).

gene (Fig. 6). Transporters of the Na^+-independent transport system, system L, and the coupling factor 4F2hc were highly expressed in DLD-1 cells.

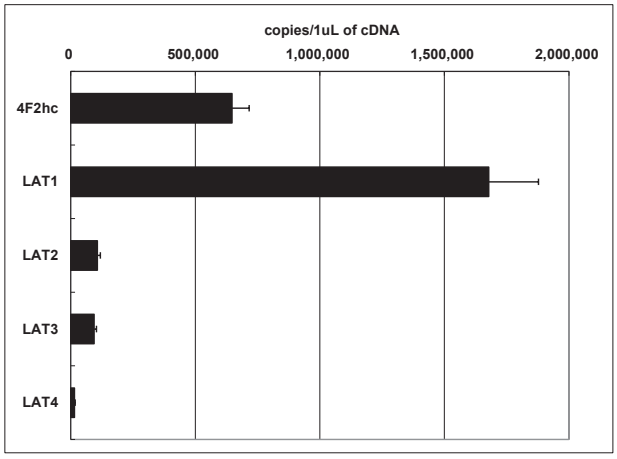

Fig. 6. Results of real-time PCR analyses.

3.5. Biodistribution Study in Mice

Following iv administration in normal mice, 6-I-D-*m*Tyr rapidly moved out of the blood and into the tissues (Table 2 A, B). The rapid decrease in the level of 6-I-D-*m*Tyr in the blood and conspicuous accumulation in the tumor tissues on imaging support its usefulness as a molecular imaging agent for tumors. Also, accumulation in the pancreas showed the characteristic *in vivo* kinetics of AAs. Almost no radioactivity accumulation was seen in the stomach, indicating high resistance of 6-I-D-*m*Tyr to

Table 2. Biodistribution of 6-I-D-*m*Tyr in normal mice.

A Biodistribution of 6-I-D-*m*Tyr in mice (% dose/g)

	2 min	5 min	10 min	15 min	30 min
Blood	6.531±0.416	3.605±0.415	2.327±0.222	1.491±0.102	0.675±0.160
Brain	0.218±0.012	0.151±0.065	0.081±0.012	0.067±0.013	0.050±0.013
Pancreas	4.528±0.298	3.594±0.304	2.368±0.274	1.977±0.648	0.594±0.151
Spleen	2.228±0.182	1.371±0.149	0.964±0.218	0.702±0.117	0.330±0.088
Stomach	0.441±0.140	0.342±0.074	0.441±0.205	0.512±0.225	0.564±0.054
Intestine	1.687±0.151	1.082±0.223	0.641±0.063	0.533±0.061	0.411±0.038
Liver	7.984±1.078	6.416±0.397	5.066±0.557	4.582±0.881	2.387±0.245
Kidney	45.321±10.681	18.706±0.432	9.770±1.243	18.543±0.462	5.274±5.037
Heart	2.874±0.226	1.372±0.340	0.828±0.078	0.770±0.143	0.365±0.097
Lung	4.349±0.331	2.391±0.248	1.565±0.207	1.413±0.204	0.667±0.113

All values are mean ± SD.

B Biodistribution of 6-I-D-*m*Tyr in mice (% dose/organ)

	2 min	5 min	10 min	15 min	30 min
Blood	2.613±0.166	1.442±0.166	0.931±0.089	0.596±0.041	0.270±0.064
Brain	0.075±0.011	0.055±0.023	0.032±0.005	0.026±0.004	0.020±0.005
Pancreas	0.586±0.150	0.535±0.093	0.364±0.076	0.254±0.060	0.078±0.008
Spleen	0.159±0.012	0.121±0.036	0.097±0.045	0.056±0.016	0.032±0.010
Stomach	0.534±0.059	0.325±0.043	0.351±0.143	0.389±0.122	0.437±0.161
Intestine	3.727±2.227	3.046±0.540	1.770±0.175	1.409±0.124	1.090±0.151
Liver	12.090±1.827	10.096±0.937	7.970±0.927	6.482±0.810	3.627±0.402
Kidney	15.472±3.392	7.155±0.524	3.543±0.845	6.671±0.597	1.905±1.851
Heart	0.343±0.057	0.161±0.063	0.082±0.005	0.076±0.021	0.036±0.008
Lung	0.689±0.067	0.423±0.063	0.325±0.139	0.261±0.019	0.136±0.022

All values are mean ± SD.

de-iodination. This suggests that it will be possible to avoid undesirable radiation exposure of the thyroid, stomach, and other organs due to the release of radioactive iodine via de-iodination reactions. There was some accumulation in the intestine and liver on a per-organ basis, but on the per-organ-weight basis this accumulation was minor. Physiologic accumulation in normal mouse tissues was low overall, and since there was little physiologic accumulation in the brain and lungs, 6-I-D-*m*Tyr may be effective for tumors in these organs.

4. Discussion

In our research into 6-I-D-*m*Tyr, we first took into consideration measurement of L-3,4-dihydroxyphenylalanine (DOPA) decarboxylase activity and developed an L-isoform (6-I-l-*m*Tyr) as a cranial nerve transmission function imaging agent for cerebral dopaminergic presynaptic function.[16] Based on the results of rat brain experiments using inhibitors, we hypothesized that 6-I-l-*m*Tyr would be useful as a diagnostic imaging agent that reflects both the activity of AA transport enzymes (for which an inhibitory effect was seen) and the level of DOPA decarboxylase activity. On the other hand, although the optical isomer of 6-I-l-*m*Tyr, 6-I-D-*m*Tyr, reflected AA transport in the same rat brain studies, we found that it did not reflect the level of DOPA decarboxylase activity. It was thus concluded that the D-isomer could not be used to quantify DOPA decarboxylase activity.

With the objective of identifying a different application for 6-I-D-*m*Tyr, in the present study, we basically examined its potential as a diagnostic imaging agent for tumors in which AA transport is said to be enhanced. First, we generated curves for 6-I-D-*m*Tyr uptake into human colon tumor DLD-1 cells over time, thereby confirming that this uptake occurs. When 4°C PBS containing Na^+ was used as the uptake solution, 6-I-D-*m*Tyr was incorporated into DLD-1 cells, and that accumulation was reduced by 71.0±5.0% in the presence of a membrane transport inhibitor. About 30% of the total uptake was estimated to be due to diffusive transport. Accordingly, we confirmed that 6-I-D-*m*Tyr accumulation in DLD-1 cells predominantly occurs via membrane transport.

As the membrane transport responsible for the accumulation of 6-I-D-*m*Tyr involves an AA transport system, we then carried out uptake inhibition experiments. Various AA membrane transport systems have been described, including transport system L, transport system A, and transport system ASC, among others. Transport systems A and ASC depend on the presence of Na^+, and they can be distinguished on the basis of specific inhibition by artificial AAs and on pH dependence. That is, transport system A is Na^+ dependent, and uptake is inhibited by the artificial AA MeAIB. Like transport system A, transport system ASC is Na^+ dependent, but it is not inhibited by MeAIB. Transport system L is independent of Na^+, and it is specifically inhibited by a different artificial AA, BCH.

In our present experiments, we examined 6-I-D-*m*Tyr uptake into DLD-1 cells to determine what kind of dependence it showed in terms of the concentration of MeAIB as a specific inhibitor of transport system A, or the concentration of BCH a specific inhibitor of transport system L. Our aim was to determine the concentration of each of those compounds to be used in inhibition experiments. We found that 6-I-D-*m*Tyr uptake into DLD-1 cells did not show any clear dependence on the concentration of MeAIB, so we decided to use this inhibitor at 1 mM in the inhibition experiments (Fig. 4-B). Conversely, the uptake of 6-I-D-*m*Tyr into DLD-1 cells was dependent on the concentration of BCH, and the amount of 6-I-D-*m*Tyr taken up decreased as the BCH concentration increased. We therefore decided on a concentration of 10 mM of this inhibitor for the uptake inhibition experiments (Fig. 4-A).

Uptake of 6-I-D-*m*Tyr did not differ significantly as a function of whether or not Na^+ was included in the PBS, leading us to conclude that neither of the Na^+-dependent transport systems (i.e., systems A and ASC) is involved in 6-I-D-*m*Tyr uptake by DLD-1 cells. It became clear that the hypothesis that transport system L is primarily responsible for 6-I-D-*m*Tyr uptake is correct (Fig. 4-C). Thus, there was no contradiction with real-time PCR results demonstrating expression of the LAT1, LAT2, LAT3, and LAT4 transporter genes of transport system L and the 4F2hc coupling factor. Cellular accumulation of

D-[^{14}C(U)]tyrosine can also be thought of as primarily due to transport system L, and a similar discussion applies (Fig. 5).

Among the isoforms of transport system L AA transporters, the LAT1 and 4F2hc heterodimers have received considerable attention in regard to tumors and activation of leukocytes.[20] It is hoped that there will be studies of 6-I-D-*m*Tyr transport and the expression of tumor-related AA transport systems other than the ones we examined in the present study, such as $B^{0,+}$, ASCT2, and xCT.[21]

We also investigated the biodistribution of 6-I-D-*m*Tyr. Following iv administration to normal mice, 6-I-D-*m*Tyr moved out of the blood and into the tissues and was rapidly eliminated from the blood (Table 2 A, B). The rapid decrease in the level of 6-I-D-*m*Tyr in the blood and conspicuous accumulation in the tumor tissues on imaging support its usefulness as a molecular imaging agent for tumors. Also, the accumulation of 6-I-D-*m*Tyr in the pancreas showed the characteristic *in vivo* kinetics of AAs. Almost no radioactivity accumulation was seen in the stomach, indicating high resistance of 6-I-D-*m*Tyr to de-iodination. This suggests that it will be possible to avoid undesirable radiation exposure of the thyroid, stomach, and other organs due to radioactive iodine (^{125}I-I^-) released by de-iodination reactions. There was some accumulation in the intestine and liver on a per-organ basis, but on the per-organ-weight basis it was minor. Physiologic accumulation in normal mouse tissues was low overall, and since there was little physiologic accumulation in the brain and lungs, 6-I-D-*m*Tyr may be effective for evaluating tumors in these organs.

In general, many tyrosine analogues show high levels of excretion in the urine, and it is therefore said that they are unsuitable for visualizing organs that are in the vicinity of the kidneys and urinary tract.[17] The accumulation rate of tyrosine analogues in the kidney is low in comparison with ^{125}I-3-alpha-methyl tyrosine (IMT).[17] It has been suggested that, at the time of testing, it is relatively advantageous to have the patient urinate as a pretreatment to eliminate radioactivity from the urinary tract, as this will improve imaging of tumors in the colon and other adjacent organs. It is hoped that studies will be carried out by administering 6-I-D-*m*Tyr to mice harboring transplanted tumors, followed by imaging for visual verification of the biodistribution.

5. Conclusion

We confirmed that DLD-1 cells accumulate 6-I-D-*m*Tyr via transport system L. Experiments in mice confirmed that 6-I-D-*m*Tyr is highly resistant to de-iodination. Moreover, the *in vivo* accumulation of 6-I-D-*m*Tyr in normal mouse tissues is low. Following administration to normal mice, the concentration of 6-I-D-*m*Tyr in various organs and tissues decreased rapidly. In contrast, 6-I-D-*m*Tyr that had accumulated inside tumor cells exhibiting enhanced expression of transport system L transporters was retained for a long time. In this situation, 6-I-D-*m*Tyr has the potential to be highly useful as a new radiopharmaceutical for molecular imaging of tumors. Further investigation is expected for molecular imaging of tumors via SPECT using 6-I-D-*m*Tyr.

Conflict of Interest

The authors declare that they have no conflict of interest.

Acknowledgement

We wish to thank Yuko Hamai, Sanae Matsutani, Naomi Tojyo, Yumi Suzuki, Yuko Hirotsu, Sayaka Imai, and Kei Satoh (Ibaraki Prefectural University of Health Sciences) for their excellent technical assistance. This work was supported by Grants-in-Aid for Scientific Research (#26461801) from the Ministry of Education, Science, Sports and Culture of Japan and the Japan Society for the Promotion of Science. Financial support was also provided by a Japan Atherosclerosis Research Foundation Grant in 2016-2018.

References

1) Kawai K, Fujibayashi Y, Saji H, Konishi J, Kubodera A, Yokoyama A. Monoiodo-D-tyrosine, an artificial amino acid radiopharmaceutical for selective measurement of membrane amino acid transport in the pancreas. Int J Rad Appl Instrum B. 1990;17:369-76.
2) Langen KJ, Hamacher K, Bauer D, Broer S, Pauleit D, Herzog H, Floeth F, Zilles K, Coenen HH. Preferred stereoselective transport of the D-isomer of cis-4-[^{18}F]fluoro-proline at the blood-brain barrier. Journal of Cerebral Blood Flow and Metabolism. 2005;25:607–16.
3) Takeda A, Goto R, Tamemasa O, Chaney JE, Digenis GA. Biological evaluation of radiolabeled D-methionine as a parent compound in potential nuclear imaging. Radioisotopes. 1984;33:213–7.
4) Tamemasa O, Goto R, Takeda A, Maruo K. High uptake of ^{14}C-labeled D-amino acids by various tumors. Gann. 1982;73:147–52.
5) Shikano N, Nakajima S, Kotani T, Ogura M, Sagara J, Iwamura Y, Yoshimoto M, Kubota N, Ishikawa N, Kawai K. Transport of D-[1-^{14}C]-amino acids into Chinese hamster ovary (CHO-K1) cells: implications for use of labeled d-amino acids as molecular imaging agents. Nucl Med Biol. 2007;34:659-65.
6) Kersemans V, Cornelissen B, Kersemans K, Bauwens M, Dierckx RA, De Spiegeleer, B, Mertens J, Slegers G. $^{123/125}$I-labelled 2-iodo-L-phenylalanine and 2-iodo-D-phenylalanine: comparative uptake in various tumour types and biodistribution in mice. Nucl Med Mol Imaging. 2006;33:919–27.
7) Bauwens M, Keyaerts M, Lahoutte T, Kersemans K, Caveliers V, Bossuyt A, Mertens J. Intra-individual comparison of the human biodistribution and dosimetry of the D and L isomers of 2-[^{123}I]iodo-phenylalanine. Nucl Med Comm. 2007;28:823–28.
8) Tsukada H, Sato K, Fukumoto D, Kakiuchi T. Evaluation of D-isomers of *O*-^{18}F-fluoromethyl, *O*-^{18}F-fluoroethyl and *O*-^{18}F-fluoropropyl tyrosine as tumour imaging agents in mice. Nucl Med Mol Imaging. 2006;33:1017–24.
9) Tsukada H, Sato K, Fukumoto D, Nishiyama S, Harada N, Kakiuchi T. Evaluation of D-isomers of *O*-^{11}C-methyl tyrosine and *O*-^{18}F-fluoromethyl tyrosine as tumor-imaging agents in tumor-bearing mice: comparison with L- and D-^{11}C-methionine. J Nucl Med. 2006;47:679–88.
10) Heiss P, Mayer S, Herz M, Wester HJ, Schwaiger M, Senekowitsch-Schmidtke
R. Investigation of transport mechanism and uptake kinetics of *O*-(2-[^{18}F]fluoroethyl)-L-tyrosine in vitro and in vivo. J Nucl Med. 1999;40:1367–73.
11) Wester HJ, Herz M, Weber W, et al. Synthesis and radiopharmacology of *O*-(2-[^{18}F]fluoroethyl)-L-tyrosine for tumor imaging. J Nucl Med. 1999;40: 205–212.
12) Schober O, Duden C, Meyer GJ, Muller JA, Hundeshagen H. Non selective transport of [^{11}C-methyl]-L- and D-methionine into a malignant glioma. Eur J Nucl Med. 1987;13:103–5.
13) Bergstro¨m M, Lundqvist H, Ericson K, et al. Comparison of the accumulation kinetics of L-(methyl-^{11}C)-methionine and D-(methyl-^{11}C)-methionine in brain tumor studies with positron emission tomography. Acta Radiol. 1987;28:225–9.
14) Kobayashi M, Hashimoto F, Ohe K, Nadamura T, Nishi K, Shikano N, Nishii R, Higashi T, Okazawa H, Kawai K.Transport mechanism of ^{11}C-labeled L- and D-methionine in human-derived tumor cells. Nucl Med Biol. 2012;39:1213-8.
15) Kawai K, Flores LG 2nd, Nakagawa M, Shikano N, Jinnouchi S, Tamura S, Kubodera A. Brain uptake of iodinated L-*meta*-tyrosine, a metabolically stable amino acid derivative. Nucl Med Commun. 1999;20:153-7.
16) Flores LG 2nd, Kawai K, Nakagawa M, Shikano N, Jinnouchi S, Tamura S, Watanabe K, Kubodera A. A new radiopharmaceutical for the cerebral dopaminergic presynaptic function: 6-radioiodinated L-*meta*-tyrosine. J Cereb Blood Flow Metab. 2000;20:207-12.
17) Shikano N, Kawai K, Flores LG 2nd, Nishii R, Kubota N, Ishikawa N, Kubodera A. An artificial amino acid, 4-iodo-L-*meta*-tyrosine: biodistribution

and excretion via kidney. J Nucl Med. 2003;44:625-31.

18) Shikano N, Kawai K, Nakajima S, Kubodera A, Kubota N, Ishikawa N, Saji H. Transcellular transport of 4-iodo-L-*meta*-tyrosine via system L across monolayers of kidney epithelial cell line LLC-PK1. Nucl Med Biol. 2004;31:477-82.

19) Dexter Daniel L., Barbosa James A., Calabresi Paul. *N,N*-Dimethylformamide-induced Alteration of Cell CultureCharacteristics and Lossof Tumorigenicity in Cultured Human Colon Carcinoma Cells, Cancer Res. 1979;39:1020-5.

20) Kanai Y, Segawa H, Miyamoto Ki, Uchino H, Takeda E, Endou H. Expression cloning and characterization of a transporter for large neutral amino acids activated by the heavy chain of 4F2 antigen (CD98). J Biol Chem. 1998;273:23629-32.

21) Wongthai P, Hagiwara K, Miyoshi Y, Wiriyasermkul P, Wei L, Ohgaki R, Kato I, Hamase K, Nagamori S, Kanai Y. Boronophenylalanine, a boron delivery agent for boron neutron capture therapy, is transported by $ATB^{0,+}$, LAT1 and LAT2. Cancer Sci. 2015;106:279-86.

和文抄録

^{123}I-6-iodo-D-*meta*-tyrosine（^{123}I-6-D-*m*Tyr）は，腫瘍分子イメージング用の放射性ヨウ素標識D-アミノ酸候補化合物である。その^{125}I標識体を用いDLD-1ヒト大腸癌株化細胞における集積のメカニズムと正常マウスにおける体内分布を検討した。DLD-1による検討では，分子デザインの母体化合物D- [^{14}C(U)] tyrosineを比較のために用いた。双方のD体アミノ酸は，約50％が中性アミノ酸輸送系Lによるものであった。正常マウスの組織における^{125}I-6-D-*m*Tyrの生理学的集積は全体的に低く，速やかな血液からのクリアランスが観察された。癌細胞とマウスによるこれらの検討から，腫瘍分子イメージングにおける新しい診断薬としての^{125}I-6-D-*m*Tyrの可能性が示唆された。